Differential expression profile analysis of DNA damage repair genes in CD133+/CD133- colorectal cancer cells

YUHONG LU[1*], XIN ZHOU[2*], QINGLIANG ZENG[2], DAISHUN LIU[3] and CHANGWU YUE[3]

[1]College of Basic Medicine, Zunyi Medical University, Zunyi; [2]Deparment of Gastroenterological Surgery, Affiliated Hospital of Zunyi Medical University, Zunyi; [3]Zunyi Key Laboratory of Genetic Diagnosis and Targeted Drug Therapy, The First People's Hospital of Zunyi, Zunyi, Guizhou 563003, P.R. China

Received July 20, 2015; Accepted January 6, 2017

DOI: 10.3892/ol.2017.6415

Abstract. The present study examined differential expression levels of DNA damage repair genes in COLO 205 colorectal cancer cells, with the aim of identifying novel biomarkers for the molecular diagnosis and treatment of colorectal cancer. COLO 205-derived cell spheres were cultured in serum-free medium supplemented with cell factors, and CD133+/CD133- cells were subsequently sorted using an indirect CD133 microbead kit. *In vitro* differentiation and tumorigenicity assays in BABA/c nude mice were performed to determine whether the CD133+ cells also possessed stem cell characteristics, in addition to the COLO 205 and CD133- cells. RNA sequencing was employed for the analysis of differential gene expression levels at the mRNA level, which was determined using reverse transcription-quantitative polymerase chain reaction. The mRNA expression levels of 43 genes varied in all three types of colon cancer cells (false discovery rate ≤0.05; fold change ≥2). Of these 43 genes, 30 were differentially expressed (8 upregulated and 22 downregulated) in the COLO 205 cells, as compared with the CD133- cells, and 6 genes (all downregulated) were differentially expressed in the COLO 205 cells, as compared with CD133+ cells. A total of 18 genes (10 upregulated and 8 downregulated) were differentially expressed in the CD133- cells, as compared with the CD133+ cells. By contrast, 6 genes were downregulated and none were upregulated in the CD133+ cells compared with the COLO 205 cells. These findings suggest that CD133+ cells may possess the same DNA repair capacity as COLO 205 cells. Heterogeneity in the expression profile of DNA damage repair genes was observed in COLO 205 cells, and COLO 205-derived CD133- cells and CD133+ cells may therefore provide a reference for molecular diagnosis, therapeutic target selection and determination of the treatment and prognosis for colorectal cancer.

Correspondence to: Dr Changwu Yue, Zunyi Key Laboratory of Genetic Diagnosis and Targeted Drug Therapy, The First People's Hospital of Zunyi, 98 Phoenix Road, Huichuan, Zunyi, Guizhou 563003, P.R. China
E-mail: changwuyue@hotmail.com

Dr Daishun Liu, Zunyi Key Laboratory of Genetic Diagnosis and Targeted Drug Therapy, The First People's Hospital of Zunyi, 98 Phoenix Road, Huichuan, Zunyi, Guizhou 563003, P.R. China
E-mail: ldsdoc@126.com

*Contributed equally

Key words: expression profile analysis, DNA damage repair, colorectal cancer

Introduction

Mammalian cells are exposed to numerous sources of DNA damage, and have therefore evolved DNA damage response signaling pathways to monitor genome integrity (1-3). In the last 30 years, a number of studies investigated the molecular mechanisms underlying the DNA damage response, and previous studies have revealed complex and profound changes in genome integrity and gene expression levels (4-6). More than 180 genes have been demonstrated to be directly or indirectly involved in the biological processes underlying DNA repair. Individuals with inherited deficiencies in the three major components involved in the DNA damage response, sensors, signal transducers and effectors have been identified (7,8). These components function by detecting several forms of DNA damage and triggering DNA damage response cascades (9). Examples of core sensors include the ataxia telangiectasia mutated (ATM) (10), ATM-Rad3-related (11) and DNA-dependent protein kinases, which are crucial to the DNA damage response signaling pathway (12,13). Signal transducers include the tumor protein p53, which has numerous roles in various DNA repair signaling pathways (14). Effectors that respond to the cellular stress of DNA damage include cyclin-dependent kinase inhibitor 1A (15), growth arrest and DNA-damage-inducible α, p53 dependent G_2 arrest mediator candidate and damage-specific DNA binding protein 2, all of which are regulated by p53 (16,17). Among the 180 genes involved in several repair signaling pathways, numerous genes are regulated by epigenetic mechanisms and are frequently downregulated or silenced in various types of cancer (18). Defects in the DNA damage response frequently occur in types of human cancer and further elucidation of this process

may facilitate the development of effective personalized cancer therapy (19-25).

In the present study, changes in the expression levels of DNA damage repair genes were determined using gene expression profile analysis through second-generation sequencing in cluster of differentiation (CD) 133^+/$CD133^-$ colorectal cancer cells (26,27). The current study, therefore, aimed to enhance the understanding of the complex gene regulation network in cancer cells and to identify novel candidate genes for cancer therapy.

Materials and methods

Cell lines, animal models and reagents. The COLO 205 human colorectal cancer cell line was obtained from the Cell Resource Center of the Shanghai Institutes for Biological Sciences, Chinese Academy of Sciences (Shanghai, China). BALB/c nude mice were obtained from the Laboratory Animal Center of Daping Hospital of the Third Military Medical University (Chongqing, China) and kept in a specific-pathogen-free animal facility. A total of twelve 5-week-old, 18-22 g specific-pathogen-free male Balb/c nude mice were purchased from the Laboratory Animal Center of Daping Hospital of the Third Military Medical University (Chongqing, China) and maintained in a pathogen-free animal facility. The study protocol was approved by Animal ethics committee of Zunyi Medical University (Zunyi, China). The present study followed guidelines of the Zunyi Medical University for Biomodel Organisms during this study.

A human CD133 MicroBead Kit (cat. no., 130-050-801) was purchased from Miltenyi Biotec GmbH (Bergisch Gladbach, Germany). B27 supplement, cell factors including recombinant human alkaline fibroblast growth factor (rh-AFGF), recombinant human epidermal cell growth factor (rh-ECGF), and recombinant human leukemia inhibitory factor (rh-LIF) and kits for RNA isolation, purification and quantification were all purchased from Invitrogen (Thermo Fisher Scientific, Inc., Waltham, MA, USA). Fetal bovine serum, media (Dulbecco's modified Eagle's medium/nutrient mixture F-12, DMEM/F-12; RPMI-1640) and trypsin were purchased from Gibco (Thermo Fisher Scientific, Inc.). Dimethyl sulfoxide and all other laboratory chemicals were purchased from Sigma-Aldrich (Merck Millipore, Darmstadt, Germany). The kits for sequencing library construction, Low Input Library Prep Kit HT (cat. no., 634900), DNA Standards for Library Quantification (cat. no., 638325) and gene expression profile analysis were obtained from Illumina, Inc. (San Diego, CA, USA). Reagents for reverse transcription-quantitative polymerase chain reaction (RT-qPCR) analysis were purchased from Takara Biotechnology Co., Ltd. (Dalian, China). The primers used for gene expression analysis (Table I) were synthesized by Invitrogen (Thermo Fisher Scientific, Inc.) and preserved in Zunyi Key Laboratory of Genetic Diagnosis & Targeted Drug Therapy.

Cell culture and isolation. These processes were performed according to previous protocol (28,29). The COLO 205 cells were maintained in RPMI-1640 supplemented with 10% fetal bovine serum until the logarithmic growth phase and were subsequently transferred to serum-free medium (SFM; DMEM/F-12 supplemented with 2% B27 supplement, 2 ng/ml recombinant human alkaline fibroblast growth factor, 2 ng/ml recombinant human epidermal cell growth factor, and 2 ng/ml recombinant human leukemia inhibitory factor) for 10 days until cell spheres formed. Cell morphology was observed by inverted fluorescence microscopy in order to detect cell adherence and growth.

Single cells separated from spheres were collected for CD133 cell isolation using a cell isolation kit (Miltenyi Biotec Inc., Shanghai, China) according to the manufacturer's protocol. Briefly, the single cell suspension was centrifuged at 800 x g for 10 min at room temperature, washed 3 times with PBS and resuspended in 300 μl isolation buffer (Miltenyi Biotec Inc., Shanghai, China). Subsequently, 100 μl FcR blocking reagent and 100 μl CD133 immunomagnetic beads (Miltenyi Biotec Inc., Shanghai, China) were added. The cell suspension was incubated at 4˚C for 30 min. The cells were washed with 2 ml isolation buffer and centrifuged at 800 x g for 10 min at room temperature followed by resuspension in 500 μl isolation buffer. An MS column (Miltenyi Biotec Inc., Shanghai, China) was washed with 500 μl isolation buffer, to which the cells were added for isolation.

Cell differentiation and tumorigenicity assay in nude mice. Upon isolation of the $CD133^+$ and $CD133^-$ cells, cell densities were adjusted to 5,000 cells/ml. For the differentiation assay, 1 ml isolated $CD133^+$ and $CD133^-$ cell suspensions were inoculated in SFM and cultured at 37˚C with 5% CO_2 for one week. Every two days, 2 ml SFM was added until differentiated cells formed under fluorescence microscope. For the tumorigenicity assay, the cells were divided into three groups including the isolated $CD133^+$ and $CD133^-$ cells and the unisolated COLO 205 cells, each were diluted with normal saline to a density of 1,000, 10,000, and 10,0000 cells/ml, respectively. Subsequently, various numbers of cells (1,000, 10000, and 10,0000) were injected into the axilla and the left groin of each nude mouse by subcutaneous injection. For the control mice, 1 ml normal saline was injected into the right groin. A total of 45 days subsequent to injection with cells or normal saline, all the animals were sacrificed via cervical dislocation.

RNA extraction, cDNA synthesis and expression profile sequencing. In total, 20 μg RNA was extracted separately from the isolated $CD133^+$ and $CD133^-$ cells and the unisolated COLO 205 cells using TRIzol® reagent (Thermo Fisher Scientific, Inc.), and mRNA was purified from total RNA using the Dynabeads® mRNA Purification kit, following the manufacturer's protocol (Thermo Fisher Scientific, Inc.). For cDNA synthesis and sequencing library construction, 5 μg RNA was processed using the TruSeq™ RNA Sample Prep kit (Illumina, Inc., San Diego, CA, USA). The library was constructed with an anchored oligo-dT primer, which initiated cDNA synthesis and added a universal primer sequence (TGCGAATT). The cDNA was polynucleotide tailed by the RT, producing a 3' overhanging tail. The cDNA was amplified by PCR with the reverse complementary sequence of the 3' overhanging tail and quantified using a TBS-380 Picogreen kit (Illumina, Inc. San Diego, CA, USA.). The library DNA was recovered using Certified Low Range Ultra Agarose (Bio-Rad Laboratories, Inc., Hercules, CA, USA). Briefly, DNA fragments were separated by agarose gel electrophoresis and the band was cut out and placed in a dissolving buffer [10 mM Tris-HCl

Table I. Primers for RT-qPCR.

Primer	Primer sequence, 5'-3'	Gene name
ActB F	CAGCAAGCAGGAGTATGACGAGT	β-actin
ActB R	GCTGTCACCTTCACCGTTCC	β-actin
BCL-11A F	GACAGGGTGCTGCGGTTGA	BCL11A
BCL-11A R	GGCTTGCTACCTGGCTGGAA	BCL11A
Zf1 F	GAGGAATGGGAACAACTGGACC	Rad 51
Zf1 R	ATTGCCTCGCCTGCTCGTC	Rad 51
P53 F	CCCTCCTCAGCATCTTATCCG	P53
P53 R	CAACCTCAGGCGGCTCATAG	P53

F, forward; R, reverse; P53, tumor protein 53; BCL-11a, B-cell lymphoma/leukemia 11A; RT-qPCR, reverse transcription quantitative polymerase chain reaction.

(pH 8.0), 1 mM EDTA and 200 mM KCl] with an equal volume of phenol. Subsequently, the mixture was frozen and thawed 3 times on dry ice. Aqueous supernatant was collected by centrifugation at 10,000 x g for 5 min at room temperature. Then, dilution buffer [100 mM Tris, 15% EtOH and 900 mM KCl (pH 6.3)] was added to the final optimized concentration [33 mM Tris, 5% EtOH and 300 mM KCl (pH 6.3)] and the DNA was precipitated by adding of isopropanol (final concentration: 40%, v/v), followed by centrifugation at 10,000 x g for 15 min at 4˚C. The pellet was washed with 70% ethanol, air-dried and dissolved in an appropriate buffer [10 mM Tris-HCl 1 mM EDTA (pH 7.6)] prior to further experiments.

Bridge amplification was performed using a cBot TruSeq PE Cluster kit v3-cBot-HS (Illumina, Inc., San Diego, CA, USA) followed by 200 cycles of DNA sequencing with a HiSeq 2000 TruSeq SBS kit v3-HS (Illumina, Inc. San Diego, CA, USA).

Gene expression profile analysis. Subsequent to sequencing, raw reads were trimmed by stripping the adaptor sequences and ambiguous nucleotides using SeqPrep (v 1.2.1; https://github.com/jstjohn/SeqPrep) and Sickle (v 0.3; https://github.com/najoshi/sickle). Following background subtraction and quantile normalization, the signal intensity values from the three group cells were exported to TopHat software (v 2.0.0-beta5; http://tophat.cbcb.umd.edu) for genome mapping, respectively. Gene expression analysis was performed using the Cuffdiff program (v 2.2.0) from the Cufflinks suite (http://cufflinks.cbcb.umd.edu) and differentially expressed genes were identified using the NOISeq workflow (v 2.16.0) in R software. Gene ontology analysis was conducted using goatools (v 0.6.10) and Kyoto Encyclopedia of Genes and Genomes (KEGG) pathway analysis was performed using KEGG-Orthhology Based Annotation System (KOBAS; v 2.1.1). For a gene to be classified as differentially expressed, Statistical significance of the gene expression model was evaluated with an ANOVA (analysis of variance) test that comparatively evaluated the variance in isolated $CD133^+$ and $CD133^-$ cells as well as the unisolated COLO 205 cells of gene expression. Differential expression was assessed using moderated t-statistics and false discovery rate <5%. $q<0.05$ was considered to indicate a statistically significant difference, whilst fold-changes were required to be >2 or <0.5.

RT-qPCR. To evaluate the differentially expressed genes observed during expression profile sequencing analysis, 11 genes were analyzed by real-time RT-qPCR using an MyiQ™ 2 Two-Color Real-Time PCR Detection system (Bio-Rad Laboratories, Inc., Hercules, CA, USA). The β-actin gene (accession number NM_0011101.3; National Center for Biotechnology Information) was used as the endogenous control. The primers (Table I) were designed using Primer Premier Software version 5.0 (Premier Biosoft International, Palo Alto, CA, USA). Total RNA (2.5 μg) was used as a template for cDNA synthesis in 50 μl RT reactions using the SuperScript® IV Reverse Transcriptase kit (Thermo Fisher Scientific, Inc.). In total, 1 μl cDNA was added into SYBR Green Real-Time PCR Master Mixes (Thermo Fisher Scientific, Inc.) for 25 μl PCR reactions. The following thermal profile was used for RT-qPCR amplification: initial denaturation for 3 min at 95˚C, followed by 40 cycles of denaturation for 10 sec at 95˚C, annealing for 30 sec at 58˚C and a thermal denaturing step from 55 to 95˚C (duration, 5 sec/0.5˚C) to generate melt curves for the determination of amplification specificity. The data were statistically analyzed using the $2^{-\Delta\Delta Cq}$ method (30).

Results

Identification of cancer stem cells. Following incubation with SFM for 1 day, the COLO 205 cells showed characteristics of low cell adherence and growth (Fig. 1A). The cells in the suspension culture demonstrated logarithmic growth and significantly increased (P=0.03) numbers of floating spheres after 5 days (Fig. 1B). After 7 days, the floating spheres began to collapse, with a small number of regular-shaped cells remaining strongly attached to one another (Fig. 1C). The surface of floating spheres appeared smoother and denser as the cell generation number increased (Fig. 1D).

Following isolation with immunomagnetic beads and culture in SFM for 1 day, the $CD133^+$ cells exhibited suspended growth, and grouped to form typical tumor spheres after 4 days, whereas spheres were absent from the $CD133^-$ cell cultures (Fig. 2A). Once fetal calf serum was added to the SFM, all the spheres derived from the $CD133^+$ cells adhered within 1 day and numerous differentiated cells with the same shape

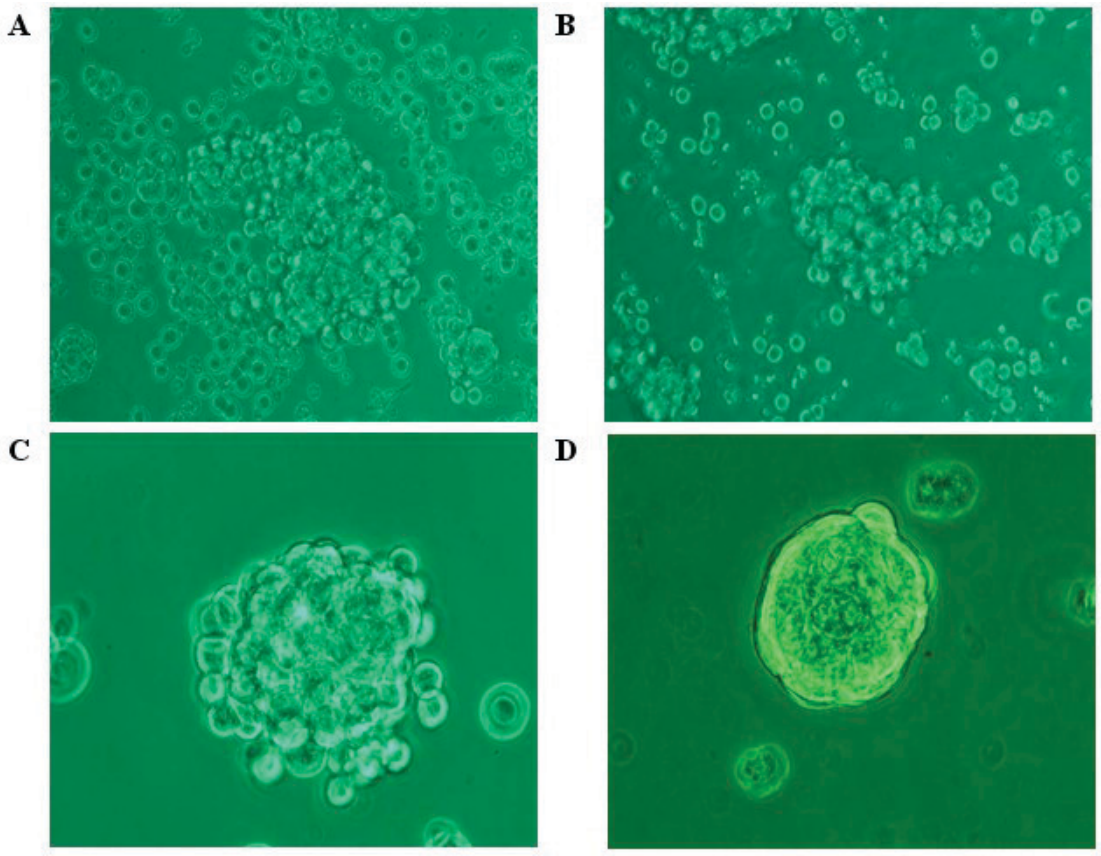

Figure 1. Human colon adenocarcinoma COLO 205 cells were cultured in serum free medium for (A) 1 day, magnification x200), (B) 5 days magnification, x200), (C) 7 days, magnification, x400 and (D) 3 generations, magnification, x400. Cells were imaged through an inverted fluorescence microscope.

as the COLO 205 cells emerged in the region surrounding the spheres after three days (Fig. 2B).

Following injection with cancer cells or normal saline, the tumor growth of the nude mice was observed and recorded daily (Fig. 3). No visible tumors were observed in the nude mice injected with the $CD133^-$ cells (Fig. 3A-a, B-a and C-a) or normal saline. In the group injected with $CD133^+$ cells, visible tumors were observed in the left axilla of all nude mice at 15, 20 and 30 days post-injection with 1,000 (Fig. 3A-b), 10,000 (Fig. 3B-b) and 100,000 cells (Fig. 3C-b). In the group injected with the COLO 205 cells, only two visible tumors were observed in the left groin of the nine nude mice 35 days post-injection with 10,000 cells (Fig. 3B-c and. C-c). Therefore, the tumorigenicity of the $CD133^+$ cells is significantly higher, compared with the $CD133^-$ cells ($P<0.01$) or COLO 205 cells ($P<0.01$), and no significant difference in tumorigenicity was observed between the $CD133^-$ cells and the COLO 205 cells ($P=0.47$).

Gene expression profiling of DNA damage repair genes. To detect changes in the mRNA expression levels of specific DNA damage repair genes in the colon cancer cells, data for the 180 genes involved in DNA repair were extracted from the results of expression profile sequencing of the isolated $CD133^+$, $CD133^-$ and COLO 205 colon cancer cells (Fig. 4).

Of these 43 genes which mRNA expression levels were altered, 30 (8 upregulated and 22 downregulated) were differentially expressed in the COLO 205 cells, as compared with the $CD133^-$ cells, and 6 genes (all downregulated) were differentially expressed in the COLO 205 cells, as compared

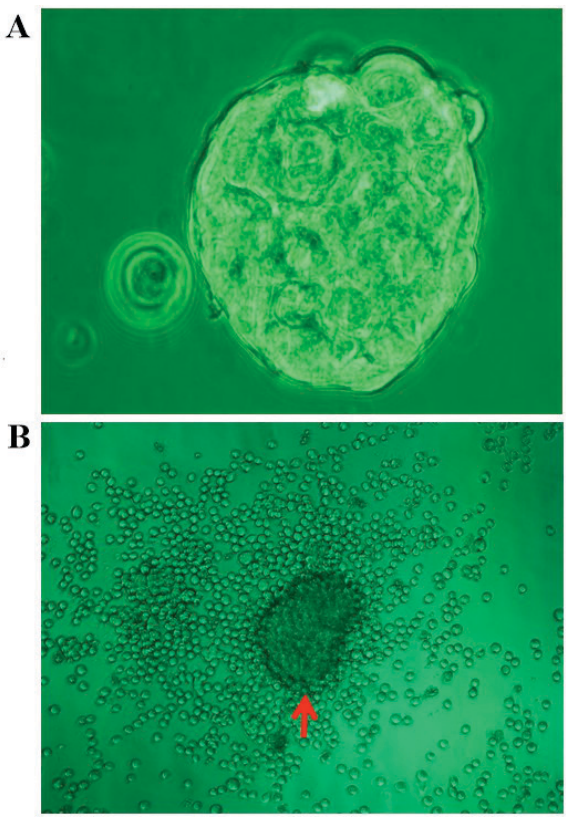

Figure 2. Differentiation of $CD133^+$ cells. (A) Sphere derived from $CD133^+$ cells (x400). (B) Differentiated cells from $CD133^+$ sphere, magnification, x100. Red arrow shows the original cell sphere.

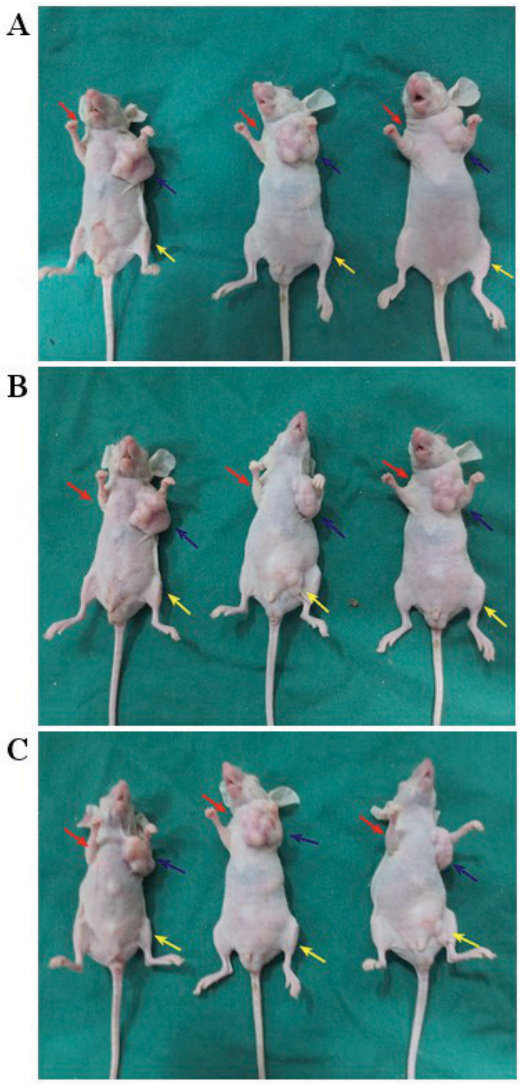

Figure 3. Analysis of tumor formation rate with various sorted cell groups at 42 days post-injection. (A) Injected with 1,000 cells. (B) Injected with 10,000 cells (C) Injected with 100,000 cells. A (red arrows), CD133$^-$ cells; b (blue arrows), CD133$^+$ cells; c (yellow arrows), COLO 205 cells.

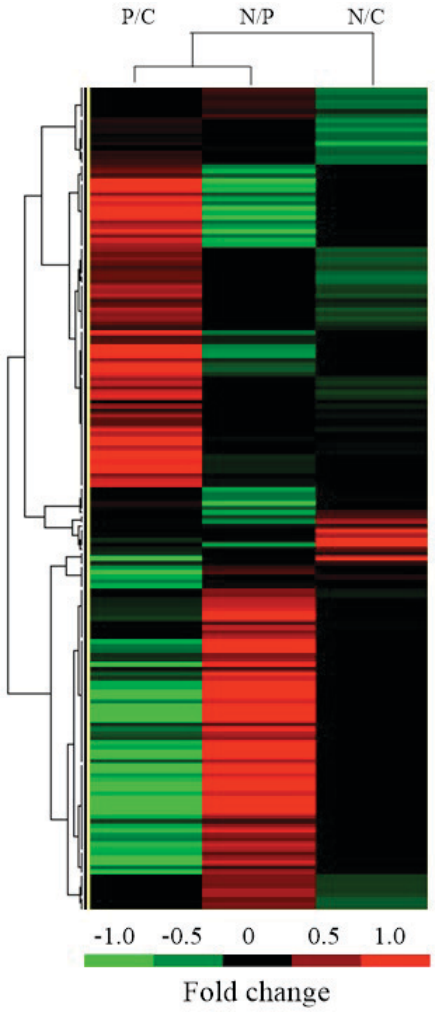

Figure 4. Gene expression profiling of DNA damage repair genes. Data (fold change) were normalized by $\log_2$ transformation. P/C, $\log_2$ [fold change (FPKM CD133$^+$/FPKM B COLO 205); N/P, $\log_2$ [fold change (FPKM CD133$^-$/FPKM CD133$^+$)]; N/C, log2 [fold change (FPKM CD133$^-$/FPKM B COLO 205)]. FKPM, fragments per kilobase of exon per million fragments mapped.

with the CD133$^+$ cells. A total of 18 genes (10 upregulated and 8 downregulated) were differentially expressed in the CD133$^-$ cells, compared with the CD133$^+$ cells. By contrast, only six genes were downregulated and none were upregulated in the CD133$^+$ cells, as compared with the COLO 205 cells. *Differential expression of DNA damage repair genes*. The results of KEGG pathway analysis revealed 14 signaling pathways that were implicated among the 40 DNA damage repair genes that were observed to be differentially expressed during the present study (Table II).

Expression analysis of differential genes. Changes in the mRNA expression levels of three genes, the conserved DNA damage response gene TP53, B-cell lymphoma/leukemia 11A (BCL-11a) and zinc-finger protein 1 (ZF1), in various cells were compared in order to examine the reliability of the results obtained from expression profile sequencing. The data were concordant between the results of the two methods of expression profile sequencing and RT-qPCR (Fig. 5). The change in the p53 mRNA expression levels in the CD133$^+$/CD133$^-$,

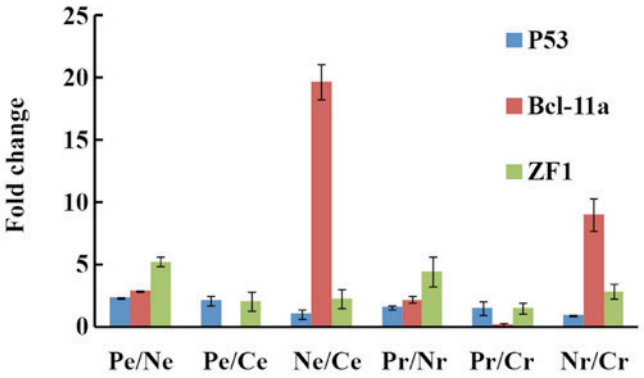

Figure 5. Gene expression analysis. Pe, expression profiling data from CD133$^+$ cells; Ne, expression profiling data from CD133$^-$ cells; Ce expression profiling data from COLO 205 cells; Pr, RT-qPCR data from CD133$^+$ cells; Nr, RT-qPCR data from CD133$^-$ cells; Cr, RT-qPCR data from COLO 205 cells; P53, tumor protein 53; BCL-1, B-cell lymphoma/leukemia 1; ZF1, zinc-finger protein 1; RT-qPCR, reverse transcription quantitative polymerase chain reaction.

Table II. Expression levels of differentially expressed genes.

Gene	Fold-change			Accession no.	Signaling pathway or function
	Pe/Ce	Ne/Pe	Ne/Ce		
UNG	0.763	0.470,	0.359, 0.19	NM_080911	Base excision repair and break joining factors
NTHL1	1.576,	0.428,	0.675,	NM_002528	Base excision repair and break joining factors
MPG	0.840,	0.553,	0.464,	NM_002434	Base excision repair and break joining factors
NEIL3	0.604,	0.554,	0.335,	NM_018248	Base excision repair and break joining factors
APEX1	0.494,	0.600,	0.297,	NM_001641	Base excision repair and break joining factors
PARP3	0.803,	0.447,	0.359,	NM_001003931	Base excision repair and break joining factors
MGMT	0.875,	0.490,	0.428,	NM_002412	Direct reversal of damage/DNA-topoisomerase crosslinks DNA-topoisomerase crosslinks DNA-topoisomerase crosslinks/DNA-topoisomerase crosslinks
ALKBH3	0.562,	0.529,	0.298,	NM_139178	Direct reversal of damage/DNA-topoisomerase crosslinks
PMS2L3	0.508,	2.305,	1.170,	NM_005395	Mismatch excision repair genes
RPA1	0.666,	0.744,	0.496,	NM_002945	NER associated genes
RPA2	0.783,	0.595,	0.465,	NM_002946	NER associated genes
GTF2H4	0.812,	0.584,	0.474,	NM_001517	NER associated genes
MNAT1	0.677,	0.529,	0.358,	NM_002431	NER associated genes
ERCC4	1.338,	1.835,	2.455,	NM_005236	NER associated genes
DMC1	1.927,	1.921,	3.702,	NM_007068	HR genes
SHFM1	1.095,	0.409,	0.448,	NM_006304	HR genes
MRE11A	0.269,	1.317,	0.355,	NM_005590	HR genes
GEN1	0.448,	2.649,	1.187,	NM_001014999	HR genes
BRIP1	0.396,	2.075,	0.822,	NM_032043	Genes involved in Fanconi anemia
FAAP20	1.318	0.410	0.540	NM_182533.2	Genes involved in Fanconi anemia
FAAP24	0.747	0.627	0.469	NM_152266	Genes involved in Fanconi anemia
XRCC6	0.591	0.778	0.460	NM_001469	Non-homologous end-joining genes
NUDT1	1.037	0.399	0.414	NM_002452	Genes involved in modulation of nucleotide pools
RRM2B	0.470	2.019	0.948	NM_015713	Genes involved in modulation of nucleotide pools
POLN	1.471	1.531	2.251	NM_181808	DNA polymerases (cofactor or catalytic subunits)
FEN1	0.589	0.849	0.500	NM_004111	Editing and processing nucleases
TREX2	0.758	0.473	0.358	NM_007205	Editing and processing nucleases
RAD18	0.593	2.696	1.598	NM_020165	Genes involved in ubiquitination and modification
HLTF	1.987	1.740	3.457	NM_003071	Genes involved in ubiquitination and modification
H2AFX	0.971	0.508	0.493	NM_002105	Genes involved in chromatin structure and modification
SETMAR	0.778	0.631	0.491	NM_006515	Genes involved in chromatin structure and modification
BLM	0.637	2.037	1.296	NM_000057	Diseases associated with sensitivity to DNA damaging agents
RPA4	0.766	0.557	0.426	NM_013347	Identified genes with DNA repair functions
PRPF19	0.451	1.637	0.739	NM_014502	Identified genes with DNA repair functions
RDM1	1.546	0.656	0.424	NM_145654	Identified genes with DNA repair functions
NABP2	0.492	0.567	0.279	NM_024068	Identified genes with DNA repair functions
ATR	1.392	1.768	2.462	NM_001184	Conserved DNA damage response genes

Table II. Continued.

Gene	Fold change			Accession no.	Signaling pathway or function
	Pe/Ce	Ne/Pe	Ne/Ce		
MDC1	0.618	6.529	4.035	NM_014641	Conserved DNA damage response genes
TP53	1.087	0.424	0.461	NM_000546	Conserved DNA damage response genes
RIF1	0.601 0.0000	2.072	1.245	NM_001177665	Conserved DNA damage response genes

Pe, Ne and Ce: mRNA expression data of $CD133^+$, $CD133^-$ and COLO 205 cells from expression profile sequencing. FKPM, fragments per kilobase of exon per million fragments mapped; UNG, uracil DNA glycosylase; NTHL1, Nth endonuclease III-Like 1; MPG, N-methylpurine DNA glycosylase; NEIL3, nei like DNA glycosylase 3; APEX1, apurinic/apyrimidinic endodeoxyribonuclease 1; PARP3, poly(ADP-ribose) polymerase family, member 3; MGMT, O^6-methylguanine DNA methyltransferase; ALKBH3, AlkB homolog 3, alpha-ketoglutarate-dependent dioxygenase; PMS2L3, PMS1 homolog 2, mismatch repair system component pseudogene 3; RPA1, replication protein A1; RPA2, replication protein A2; GTF2H4, general transcription factor IIH subunit 4; MNAT1, cyclin dependent kinase activating kinase assembly factor; ERCC4, excision repair cross-complementation group 4; DMC1, DNA meiotic recombinase 1; SHFM1, split hand/foot malformation (ectrodactyly) type 1; MRE11A, meiotic recombination 11 homolog A; GEN1, Holliday junction 5' flap endonuclease; BRIP1, breast cancer A interacting protein C-terminal helicase 1; FAAP20, fanconi anemia core complex associated protein 20; FAAP24, fanconi anemia core complex associated protein 24; XRCC6, X-ray repair cross-complementing protein 6; NUDT1, nudix hydrolase 1; RRM2B, ribonucleotide reductase regulatory tumor protein 53 inducible subunit M2B; POLN, polymerase (DNA) Nu; FEN1, flap structure-specific endonuclease 1; TREX2, three prime repair exonuclease 2; RAD18, E3 ubiquitin protein ligase; HLTF, helicase-like transcription factor; H2AFX, H2A histone family member X; SETMAR, SET domain and mariner transposase fusion; BLM, bloom syndrome protein; RPA4, replication protein A 30 kDa subunit; PRPF19, Pre-mRNA processing factor 19; RDM1, RAD52 motif containing 1; OBFC2B, nucleic acid binding protein 2; ATR, ataxia telangiectasia and Rad3 related; MDC1, mediator of DNA damage checkpoint protein 1; TP53, tumor protein 53; RIF1, replication timing regulatory factor 1; NER, Nucleotide excision repair; HR, homologous recombination.

$CD133^+$/COLO 205 and $CD133^-$/COLO 205 cells was 2.37, 2.17 and 1.09 folds, respectively, from expression profile sequencing and 1.61, 1.60 and 1.00 fold, respectively, from RT-qPCR. Similar trends in expression levels were observed in the $CD133^+$/$CD133^-$, $CD133^+$/COLO 20 and $CD133^-$/COLO 205 cells for BCL-11a (expression profile sequencing, 2.95, 0.15 and 19.67 fold; RT-qPCR, 2.25, 0.25 and 9 fold, respectively) and ZF1 (expression profile sequencing, 5.27, 2.12 and 2.36 fold; RT-qPCR, 4.53, 1.58 and 2.87 fold, respectively).

Discussion

Of the 12 genes involved in base excision repair and break joining, no variation in gene expression levels was observed in the $CD133^-$ cells, as compared with the $CD133^+$ cells; however, the expression levels of four genes were downregulated in the $CD133^-$ cells, compared with the COLO 205 cells, and the expression levels of three genes were downregulated in the $CD133^-$ cells, compared with the $CD133^+$ cells. Of these genes, uracil-DNA glycosylase and poly (adenosine diphosphate-ribose) polymerase 3 were downregulated in the COLO 205 cells and the $CD133^+$ cells. In $CD133^-$ cells, nth endonuclease III-like 1, N-methylpurine DNA glycosylase, nei endonuclease VIII-like 1 and apurinic/apyrimidinic endodeoxyribonuclease 1 were downregulated, compared with the $CD133^+$ cells. As those genes that were downregulated in expression are all involved in base excision repair (31) or break joining (32), their downregulation may have negative effects on the base excision repair capacity towards damaged DNA in $CD133^-$ cells.

A total of five human genes are involved in the direct reversal of DNA damage (33), including two tyrosyl-DNA phosphodiesterases, two alpha-ketoglutarate-dependent dioxygenases, and an O^6-methylguanine-DNA methyltransferase (MGMT). No changes in the expression levels of these five genes were observed in the $CD133^+$ cells, compared with the COLO 205 cells. By contrast, *MGMT* gene expression was upregulated in the COLO 205 cells, compared with the $CD133^-$ cells. Similarly, alkylation repair homolog 3 expression was downregulated in the $CD133^-$ cells compared with the COLO 205 cells.

By contrast, no marked changes in the expression levels of the ten genes involved in the mismatch excision repair signaling pathway were detected in all three types of cells, with the exception of postmeiotic segregation increased 2-like protein 3, which was upregulated in the $CD133^-$ cells, compared with the $CD133^+$ cells.

Nucleotide excision repair (NER) is a complex biological process, involving more than 29 genes that are able to correct DNA damage through nuclease cleavage of the damaged base, removal of the damaged oligonuclotide and resynthesis using the undamaged strand as the template (34). No significant changes in gene expression levels were observed in the $CD133^+$ cells compared with the COLO 205 cells and the $CD133^-$ cells. By contrast, five genes were differentially expressed, with the expression of four genes downregulated and upregulated for one gene in the $CD133^-$ cells, compared with COLO 205 cells.

Replication protein A1 (RPA1) and replication protein A2 (RPA2) are components of the alternative RPA complex, which is essential for the binding and stabilizing of single-stranded DNA intermediates, preventing the reannealing of complementary DNA (35). Therefore, downregulation of the expression of these two genes may reduce the NER capacity of $CD133^-$ cells. As components of the seven

subunits, as well as kinase subunits of general transcription factor IIH, downregulation of general transcription factor IIH subunit 4 and CDK-activating kinase assembly factor *MAT1* expression levels may also reduce the NER capacity (36) of $CD133^-$ cells. As excision repair cross-complementing rodent repair deficiency complementation group 4 (ERCC4) forms a complex with ERCC1 and is involved in the 5' incision made during NER (37), upregulating *ERCC4* expression may affect the nucleotide excision repair capacity of $CD133^-$ cells.

More than 19 genes are involved in homologous recombination repair (38) and, in the present study, only 4 of these genes were differentially expressed. As a component of the Mre11-Rad50-Nbs1 (MRN) complex, meiotic recombination 11 homolog A (MRE11A) exhibits single-strand endonuclease activity and double-strand 3'-5' exonuclease activity specific to the MRN complex, which is critical to the processes of double-strand break (DSB) repair, DNA recombination, maintenance of telomere integrity and meiosis (39). The expression levels of the *MRE11A* gene were downregulated in the $CD133^+$ cells and the $CD133^-$ cells, as compared with the COLO 205 cells. The Holliday junction 5' flap endonuclease, which possesses Holliday junction resolvase activity *in vitro* and is considered to function in homology-driven repair of DNA DSBs (40), exhibited upregulated expression levels in the $CD133^-$ and COLO 205 cells, as compared with the $CD133^+$ cells. Upregulated expression of the BRCA2-associated split hand/foot malformation (ectrodactyly) type 1 gene was observed in the $CD133^-$ cells, compared with the $CD133^+$ and COLO 205 cells. DNA meiotic recombinase 1, which assembles at the sites of programmed DNA DSBs and searching for allelic DNA sequences located on homologous chromatids during homologous recombination in the process of meiosis, exhibited upregulated expression in the $CD133^-$ cells, compared with the COLO 205 cells.

Of the 17 genes involved in Fanconi anemia, only three genes exhibited changes in expression levels during the present study. These were as follows: Breast cancer 1 (BRCA1)-interacting protein 1 (BRIP1), involved in the repair of DNA DSBs by BRCA1-dependent homologous recombination (41); the 20 kDa Fanconi anemia-associated protein (FAAP20), a component of the Fanconi anemia complex that is required to recruit the complex to DNA interstrand cross-links to promote repair; the 24 kDa Fanconi anemia-associated protein (FAAP24), which regulates Fanconi anemia group D2 protein monoubiquitination upon DNA damage (42). Seven genes have been reported to be involved in non-homologous end-joining (43), among them, X-ray repair cross complementing 6 (XRCC6) (44), the 70 kDa subunit of the single-stranded DNA-dependent ATP-dependent helicase II was the only one which gene expression level was changed in $CD133^+$ cells compared with $CD133^-$ cells and COLO 205 cells. Downregulation of XRCC6 expression levels (2.173 folds) in $CD133^-$ cells, compared with COLO 205 cells, may have a negative effect on the non-homologous end joining capacity of $CD133^-$ cells.

Three genes are involved in the modulation of nucleotide pools during the process of DNA damage repair in human cells (45). As an antimutagen, nucleoside diphosphate linked moiety X-type motif 1 (NUDT1) hydrolyzes oxidized purine nucleoside triphosphates, preventing the misincorporation of nucleotides (46). Downregulation of *NUDT1* expression levels in $CD133^-$ cells may reduce their capacity to sanitize oxidized nucleotide pools and increase the risk of misincorporation. In addition, the small subunit 2 of the p53-inducible ribonucleotide reductase catalyzes the conversion of ribonucleoside diphosphates to deoxyribonucleoside diphosphates (47). Therefore, the downregulated expression of the ribonucleotide reductase regulatory TP53 inducible subunit M2B in the $CD133^+$ cells, as compared with the $CD133^-$ and COLO 205 cells, may increase cell survival by promoting p53-dependent damage repair and supplying deoxyribonucleotides for DNA damage repair in cells arrested at the G_1 or G_2 phases of the cell cycle (48).

Although 17 DNA polymerases are involved in DNA damage repair as cofactors or catalytic subunits, only DNA polymerase N (*POLN*) expression was upregulated in the $CD133^-$ cells, as compared with the COLO 205 cells. As POLN is involved in the repair of DNA crosslinks (49), a change in its expression levels may affect the DNA repair capacity of $CD133^-$ cells.

Of the seven editing and processing nucleases involved in DNA damage repair (50), the expression levels of flap structure-specific endonuclease 1 (*FEN1*) and three prime repair exonuclease 2 (*TREX2*) were downregulated by 2 fold in the $CD133^-$ cells, as compared with the COLO 205 cells, and the expression of *TREX2* was downregulated in the $CD133^-$ cells, compared with the $CD133^+$ cells (2.11 folds) and the COLO 205 cells (2.79 folds). Since FEN1 and TREX2 are involved in DNA replication and mismatch repair, possessing a structure-specific nuclease activity preference for double-stranded DNA with mismatched 3'termini and 5'-flap structures (51). Therefore, downregulation of the mRNA expression levels of the two enzymes may affect the fidelity of DNA replication in human cells, which can affect the viability of cells.

Among the 11 genes involved in ubiquitination and post-translational protein modification (52) in human cells, only two genes (*RAD18* and *HLTF*) exhibited upregulated expression levels in the $CD133^-$ cells, as compared with the $CD133^+$ and COLO 205 cells. E3 ubiquitin-protein ligase RAD18, which is involved in the post-replication repair of UV-damaged DNA, and helicase-like transcription factor, which functions in the error-free post-replication repair of damaged DNA and the maintenance of genomic stability (53). HLTF is a SWI2/SNF2-family ATP-dependent chromatin remodeling enzyme that acts in the error-free branch of DNA damage tolerance (DDT), a cellular mechanism that enables replication of damaged DNA while leaving damage repair for a later time (54). Alterations in the expression levels of these genes may affect the cellular DNA damage repair capacity.

Three genes are known involved in chromatin structure and modification including chromatin assembly factor 1 subunit A (*CHAF1A*), H2A histone family member X (*H2AFX*) as well as SET domain and mariner transposase fusion gene (*SETMAR*). In $CD133^-$ cells, the *SETMAR* and *H2AX* genes showing the same downregulated trends in mRNA expression levels compared with the COLO 205 cells and $CD133^+$ cells. Because of H2AX has previously been demonstrated to interact with several types of cancer-associated genes, including mediator of DNA damage checkpoint protein 1 (MDC1), nibrin, tumor protein p53 binding protein 1, bloom syndrome protein, *BRCA1*, BRCA1-associated RING domain protein 1 and γ-H2AX (phosphorylated on serine 139) (55,56), and is, therefore, a sensitive target for

locating DSBs in cells. SETMAR specifically methylates histone H3 at lysines 4 and 36 and, therefore, has a role in DNA repair activities, including non-homologous end joining and DSB repair (57). Downregulation of the expression of *SETMAR* and *H2AX* may, therefore, serve a role in DNA damage though chromatin remodeling.

The five genes including Bloom syndrome RecQ like helicase (*BLM*) , Werner syndrome RecQ like helicase (*WRN*), RecQ like helicase 4 (*RECQL4*), ATM serine/threonine kinase (*ATM*) as well as M-Phase specific PLK1 interacting protein (*MPLKIP*) that are defective in diseases associated with a sensitivity to DNA damaging agents (58,59), only the Bloom syndrome helicase gene, involved in the 5' end resection of DNA during DSB repair, exhibited upregulated expression levels in the $CD133^-$ cells, as compared with the $CD133^+$ cells.

Of the nine genes that have established or suspected DNA repair functions such as DNA cross-link repair 1A (*DCLRE1A*), DNA cross-link repair 1B (*DCLRE1B*), pre-mRNA processing factor 19 (*PRPF19*), replication protein A 30 kDa subunit (*RPA4*), RecQ like helicase (*RECQL*), RecQ like helicase 5 (*RECQL5*), Helicase, POLQ-like (*HELQ*), RAD52 motif containing 1 (*RDM1*) as well as nucleic acid binding protein 2 (*NABP2*), the expression of three genes were changed. The mRNA expression levels of *RPA4* and *RDM1* were downregulated in $CD133^-$ cells compared with the COLO 205 cells and $CD133^+$ cells while *PRPF19* and *NABP2* were downregulated in $CD133^+$ cells compared with the COLO 205 cells and $CD133^-$ cells.

Of the 15 conserved DNA damage response genes (60) including ATR serine/threonine kinase (*ATR*), ATR interacting protein (*ATRIP*), mediator of DNA damage checkpoint 1 (*MDC1*), RAD1 checkpoint DNA exonuclease (*RAD1*), RAD9 checkpoint clamp component A (*RAD9A*), HUS1 checkpoint clamp component (*HUS1*), RAD17 checkpoint clamp loader component (*RAD17*), checkpoint kinase 1 (*CHEK1*), checkpoint kinase 2 (*CHEK2*), tumor protein P53 (*TP53*), tumor protein P53 binding protein 1 (*TP53BP1*), replication timing regulatory factor 1 (*RIF1*), CDC like kinase 2 (*CLK2*) and *PER1* (period circadian clock 1), the expression of *ATR* and *MDC1* were upregulated and *TP53* expression was downregulated in the $CD133^-$ cells, compared with the COLO 205 cells, whereas *RIF1* and *MDC1* expression levels were upregulated; TP53 exhibited downregulated expression levels in the $CD133^-$ cells, compared with the $CD133^+$ cells.

In conclusion, the present study demonstrated that the mRNA expression levels of 43 genes varied in all three types of colon cancer cells. Heterogeneity in the gene expression profiles of DNA damage repair genes was present in the COLO 205 cells, and in the COLO 205-derived $CD133^-$ cells and $CD133^+$ cells. The results of the present study may provide a reference for molecular diagnosis, therapeutic target selection, determination of treatment and prognostic judgment in colorectal cancer (61).

Acknowledgements

This study was supported by the Foundation of Guizhou Province Social Development of Science and Technology Research Projects [grant no. (2009) 3068)] and the Foundation of Guizhou Province Commission of Health and Family Planning [grant no. gzwjkj2015-1-045].

References

1. Zhou BB and Elledge SJ: The DNA damage response: Putting checkpoints in perspective. Nature 408: 433-439, 2000.
2. Gasser S and Raulet D: The DNA damage response, immunity and cancer. Semin Cancer Biol 16: 344-347, 2006.
3. Mallette FA and Ferbeyre G: The DNA damage signaling pathway connects oncogenic stress to cellular senescence. Cell Cycle 6: 1831-1836, 2007.
4. Liang Y, Lin SY, Brunicardi FC, Goss J and Li K: DNA damage response pathways in tumor suppression and cancer treatment. World J Surg 33: 661-666, 2009.
5. Morgan MA and Lawrence TS: Molecular pathways: Overcoming radiation resistance by targeting DNA damage response pathways. Clin Cancer Res 21: 2898-2904, 2015.
6. Shimizu I, Yoshida Y, Suda M and Minamino T: DNA damage response and metabolic disease. Cell Metab 20: 967-977, 2014.
7. Rajewsky MF, Engelbergs J, Thomale J and Schweer T: DNA repair: Counteragent in mutagenesis and carcinogenesis- accomplice in cancer therapy resistance. Mutat Res 462: 101-105, 2000.
8. Goldstein M and Kastan MB: The DNA damage response: Implications for tumor responses to radiation and chemotherapy. Annu Rev Med 66: 129-143, 2015.
9. Annovazzi L, Caldera V, Mellai M, Riganti C, Battaglia L, Chirio D, Melcarne A and Schiffer D: The DNA damage/repair cascade in glioblastoma cell lines after chemotherapeutic agent treatment. Int J Oncol 46: 2299-2308, 2015.
10. Paull TT: Mechanisms of ATM activation. Annu Rev Biochem 84: 711-738, 2015.
11. Suvorova II, Kozhukharova IV, Nikol'skiĭ NN and Pospelov VA: ATM/ATR signaling pathway activation in human embryonic stem cells after DNA damage. Tsitologiia 55: 841-851, 2013 (In Russian).
12. Kühne C, Tjörnhammar ML, Pongor S, Banks L and Simoncsits A: Repair of a minimal DNA double-strand break by NHEJ requires DNA-PKcs and is controlled by the ATM/ATR checkpoint. Nucleic Acids Res 31: 7227-7737, 2003.
13. Knittel G, Liedgens P and Reinhardt HC: Targeting ATM-deficient CLL through interference with DNA repair pathways. Front Genet 6: 207, 2015.
14. Nakazawa K, Dashzeveg N and Yoshida K: Tumor suppressor p53 induces miR-1915 processing to inhibit Bcl-2 in the apoptotic response to DNA damage. FEBS J 281: 2937-2944, 2014.
15. Mlynarczyk C and Fåhraeus R: Endoplasmic reticulum stress sensitizes cells to DNA damage-induced apoptosis through p53-dependent suppression of p21 (CDKN1A). Nat Commun 5: 5067, 2014.
16. Yajima N, Wada R, Matsuzaki Y and Yagihashi S: DNA damage response and its clinicopathological relationship in appendiceal tumors. Int J Colorectal Dis 29: 1349-1354, 2014.
17. Sun T and Cui J: A plausible model for bimodal p53 switch in DNA damage response. FEBS Lett 588: 815-821, 2014.
18. Broustas CG and Lieberman HB: DNA damage response genes and the development of cancer metastasis. Radiat Res 181: 111-130, 2014.
19. Hosoya N and Miyagawa K: Targeting DNA damage response in cancer therapy. Cancer Sci 105: 370-388, 2014.
20. Kelley MR, Logsdon D and Fishel ML: Targeting DNA repair pathways for cancer treatment: what's new? Future Oncol 10: 1215-1237, 2014.
21. Khanna A: DNA damage in cancer therapeutics: A boon or a curse? Cancer Res 75: 2133-2138, 2015.
22. Korwek Z and Alster O: The role of the DNA damage response in apoptosis and cell senescence. Postepy Biochem 60: 248-262, 2014 (In Polish).
23. Prakash A and Doublié S: Base excision repair in the mitochondria. J Cell Biochem 116: 1490-1499, 2015.
24. Tian H, Gao Z, Li H, Zhang B, Wang G, Zhang Q, Pei D and Zheng J: DNA damage response-a double-edged sword in cancer prevention and cancer therapy. Cancer Lett 358: 8-16, 2015.
25. Wallace NA and Galloway DA: Manipulation of cellular DNA damage repair machinery facilitates propagation of human papillomaviruses. Semin Cancer Biol 26: 30-42, 2014.
26. Zhou L, Wei X, Cheng L, Tian J and Jiang JJ: CD133, one of the markers of cancer stem cells in Hep-2 cell line. Laryngoscope 117: 455-460, 2007.

27. Gussin HA, Sharma AK and Elias S: Culture of endothelial cells isolated from maternal blood using anti-CD105 and CD133. Prenat Diagn 24: 189-193, 2004.
28. Yu SC, Ping YF, Yi L, Zhou ZH, Chen JH, Yao XH, Gao L, Wang JM and Bian XW: Isolation and characterization of cancer stem cells from a human glioblastoma cell line U87. Cancer Lett 265: 124-134, 2008.
29. Li HZ, Yi TB and Wu ZY: Suspension culture combined with chemotherapeutic agents for sorting of breast cancer stem cells. BMC Cancer 8: 135, 2008.
30. Ballester M, Castelló A, Ibáñez E, Sánchez A and Folch JM: Real-time quantitative PCR-based system for determining transgene copy number in transgenic animals. Biotechniques 37: 610-613, 2004.
31. Krokan HE and Bjørås M: Base excision repair. Cold Spring Harb Perspect Biol 5: a012583, 2013.
32. Lieber MR: The mechanism of human nonhomologous DNA end joining. J Biol Chem 283: 1-5, 2008.
33. Yi C and He C: DNA repair by reversal of DNA damage. Cold Spring Harb Perspect Biol 5: a012575, 2013.
34. Bowden NA: Nucleotide excision repair: Why is it not used to predict response to platinum-based chemotherapy? Cancer Lett 346: 163-171, 2014.
35. Deng SK, Chen H and Symington LS: Replication protein A prevents promiscuous annealing between short sequence homologies: Implications for genome integrity. Bioessays 37: 305-313, 2015.
36. Zhu Q, Wani G, Sharma N and Wani A: Lack of CAK complex accumulation at DNA damage sites in XP-B and XP-B/CS fibroblasts reveals differential regulation of CAK anchoring to core TFIIH by XPB and XPD helicases during nucleotide excision repair. DNA Repair (Amst) 11: 942-950, 2012.
37. McDaniel LD and Schultz RA: XPF/ERCC4 and ERCC1: Their products and biological roles. Adv Exp Med Biol 637: 65-82, 2008.
38. Prakash R, Zhang Y, Feng W and Jasin M: Homologous recombination and human health: The roles of BRCA1, BRCA2, and associated proteins. Cold Spring Harb Perspect Biol 7: a016600, 2015.
39. Borde V and Cobb J: Double functions for the Mre11 complex during DNA double-strand break repair and replication. Int J Biochem Cell Biol 41: 1249-1253, 2009.
40. Sarbajna S and West SC: Holliday junction processing enzymes as guardians of genome stability. Trends Biochem Sci 39: 409-419, 2014.
41. Li S, Ting NS, Zheng L, Chen PL, Ziv Y, Shiloh Y, Lee EY and Lee WH: Functional link of BRCA1 and ataxia telangiectasia gene product in DNA damage response. Nature 406: 210-215, 2000.
42. Koczorowska AM, Białkowska A, Kluzek K and Zdzienicka MZ: The role of the Fanconi anemia pathway in DNA repair and maintenance of genome stability. Postepy Hig Med Dosw (Online) 68: 459-472, 2014.
43. Radhakrishnan SK, Jette N and Lees-Miller SP: Non-homologous end joining: Emerging themes and unanswered questions. DNA Repair (Amst) 17: 2-8, 2014.
44. Fell VL and Schild-Poulter C: The Ku heterodimer: Function in DNA repair and beyond. Mutat Res Rev Mutat Res 763: 15-29, 2015.
45. Garre P, Briceño V, Xicola RM, Doyle BJ, de la Hoya M, Sanz J, Llovet P, Pescador P, Puente J, Díaz-Rubio E, *et al*: Analysis of the oxidative damage repair genes NUDT1, OGG1, and MUTYH in patients from mismatch repair proficient HNPCC families (MSS-HNPCC). Clin Cancer Res 17: 1701-1712, 2011.
46. Mishima M, Sakai Y, Itoh N, Kamiya H, Furuichi M, Takahashi M, Yamagata Y, Iwai S, Nakabeppu Y and Shirakawa M: Structure of human MTH1, a Nudix family hydrolase that selectively degrades oxidized purine nucleoside triphosphates. J Biol Chem 279: 33806-33815, 2004.
47. Pontarin G, Ferraro P, Håkansson P, Thelander L, Reichard P and Bianchi V: p53R2-dependent ribonucleotide reduction provides deoxyribonucleotides in quiescent human fibroblasts in the absence of induced DNA damage. J Biol Chem 282: 16820-16828, 2007.
48. Link PA, Baer MR, James SR, Jones DA and Karpf AR: p53-inducible ribonucleotide reductase (p53R2/RRM2B) is a DNA hypomethylation-independent decitabine gene target that correlates with clinical response in myelodysplastic syndrome/acute myelogenous leukemia. Cancer Res 68: 9358-9366, 2008.
49. Takata K, Tomida J, Reh S, Swanhart LM, Takata M, Hukriede NA and Wood RD: Conserved overlapping gene arrangement, restricted expression, and biochemical activities of DNA polymerase ν (POLN). J Biol Chem 290: 24278-24293, 2015.
50. Zheng L and Shen B: Okazaki fragment maturation: Nucleases take centre stage. J Mol Cell Biol 3: 23-30, 2011.
51. Mason PA and Cox LS: The role of DNA exonucleases in protecting genome stability and their impact on ageing. Age (Dordr) 34: 1317-1340, 2012.
52. Dianov GL, Meisenberg C and Parsons JL: Regulation of DNA repair by ubiquitylation. Biochemistry (Mosc) 76: 69-79, 2011.
53. Hedglin M and Benkovic SJ: Regulation of Rad6/Rad18 activity during DNA damage tolerance. Annu Rev Biophys 44: 207-228, 2015.
54. Hishiki A, Hara K, Ikegaya Y, Yokoyama H, Shimizu T, Sato M and Hashimoto H: Structure of a novel DNA-binding domain of helicase-like transcription factor (HLTF) and its functional implication in DNA damage tolerance. J Biol Chem 290: 13215-13223, 2015.
55. Cook PJ, Ju BG, Telese F, Wang X, Glass CK and Rosenfeld MG: Tyrosine dephosphorylation of H2AX modulates apoptosis and survival decisions. Nature 458: 591-596, 2009.
56. Turinetto V and Giachino C: Multiple facets of histone variant H2AX: A DNA double-strand-break marker with several biological functions. Nucleic Acids Res 43: 2489-2498, 2015.
57. Fnu S, Williamson EA, De Haro LP, Brenneman M, Wray J, Shaheen M, Radhakrishnan K, Lee SH, Nickoloff JA and Hromas R: Methylation of histone H3 lysine 36 enhances DNA repair by nonhomologous end-joining. Proc Natl Acad Sci USA 108: 540-545, 2011.
58. Frank B, Hoffmeister M, Klopp N, Illig T, Chang-Claude J and Brenner H: Colorectal cancer and polymorphisms in DNA repair genes WRN, RMI1 and BLM. Carcinogenesis 31: 442-445, 2010.
59. Nimonkar AV, Genschel J, Kinoshita E, Polaczek P, Campbell JL, Wyman C, Modrich P and Kowalczykowski SC: BLM-DNA2-RPA-MRN and EXO1-BLM-RPA-MRN constitute two DNA end resection machineries for human DNA break repair. Genes Dev 25: 350-362, 2011.
60. Strzyz P: DNA damage response: Cell thriving despite DNA damage. Nat Rev Mol Cell Biol 17: 396, 2016.
61. Lord CJ and Ashworth A: The DNA damage response and cancer therapy. Nature 481: 287-294, 2012.